Supporting information

High stability of the He atom confined in a U@C_{60} fullerene

Yanyu Lei,[a,b] Bo Wang,[a,b] Yang Gao, [a,b] Wanrun Jiang, [a,b] Dexuan Xu,[a,b] Wei Zhang[c,*] and Zhigang Wang[a,b,d,*]

[a]Institute of Atomic and Molecular Physics, Jilin University, Changchun 130012, P. R. China,

[b]Jilin Provincial Key Laboratory of Applied Atomic and Molecular Spectroscopy (Jilin University), Changchun, 130012, P. R. China.

[c]Shanghai Institute of Applied Physics, Chinese Academy of Sciences, Shanghai 201800, P. R. China

[d]Institute of Theoretical Chemistry, Jilin University, Changchun 130023, P. R. China

Correspondence and requests for materials should be addressed to Zhigang Wang (wangzg@jlu.edu.cn), and Wei Zhang (zhangwei@sinap.ac.cn).

Contents

Part 1. The calculated energies of UHe@C_{60}

Part 2.The related information for U_2@C_{60} and U_2@C_{61}

Part 3. Relative energy calculations for UHe@C_{60} using ZORA approach

Part 4. Molecular dynamics simulations of UHe@C_{60}

Part 5. Charge distribution and spin population of UHe@C_{60} and U@C_{60}

Part 6. Contour maps of electron density difference for UHe@C_{60}

Part 7. Detailed data of energy decomposition analysis for UHe@C_{60} system

Part 8. Detailed data of TD-DFT calculations for UHe@C_{60}

Part 9. Infrared and Raman spectra of UHe@C_{60} and U@C_{60}

Part 1. The calculated energies of UHe@C_{60}

Table S1. The calculated total energies of UHe@C_{60} with different configurations and various spin multiplicities. The results with ZPE corrections are also included in brackets. All the final geometries have no imaginary frequency and their energies are given in Hartree.

Multiplicity	final structure	E_{bond}	E_{R6}	E_{atom}	E_{R5}
Singlet	UHe@C_{60} (R_6)	-2763.41286 (-2763.04810)	-2763.41284 (-2763.04809)	-2763.41278 (-2763.04807)	-2763.41280 (-2763.04810)
Triplet	**UHe@C_{60} (R_6)**	**-2763.42516 (-2763.06080)**	**-2763.42516 (-2763.06079)**	**-2763.42513 (-2763.06069)**	**-2763.42516 (-2763.06069)**
Quintet	UHe@C_{60} (B)	-2763.40560 (-2763.04264)	-2763.40560 (-2763.04264)	-2763.40560 (-2763.04263)	-2763.405602 (-2763.04265)
Septet	UHe@C_{60} (A)	-2763.38207 (-2763.01899)	-2763.38208 (-2763.01896)	-2763.38210 (-2763.01898)	-2763.38209 (-2763.01892)

Part 2. The related information for U_2@C_{60} and U_2@C_{61}.

We used the benchmark calculations on U_2@C_{60} and U_2@C_{61} at PBE/SEG_ECP60MWB~6-31G (d) level to show the results are reliable. For the U_2@C_{60} and U_2@C_{61}, we calculated the data on bond length, IR and Raman spectra, respectively. These results are all listed in the following, which are consistent with the previous theoretical research.[24,48] For example, both U_2@C_{60} and U_2@C_{61} have two types of stretching modes, i.e., symmetric and asymmetric modes. The symmetric U-U stretching mode is IR-inactive, but while the asymmetric U-U stretching is Raman-inactive. Thus, these comparisons confirm the reliability of our current method.

Table S2. Calculated information of U_2@C_{60} and U_2@C_{61}.

Property	U_2@C_{60}[a]	U_2@C_{60}[c]	U_2@C_{61}[b]	U_2@C_{61}[c]
U-U bond length (Å)	2.72	2.74	2.80	2.84
stretching modes (cm^{-1})				
symmetric	168.7	148.6	127.4	116.2
Asymmetric	147.4	156.1	142.0	141.3

[a] Ref [24] [b] Ref [48] [c] Our calculations.

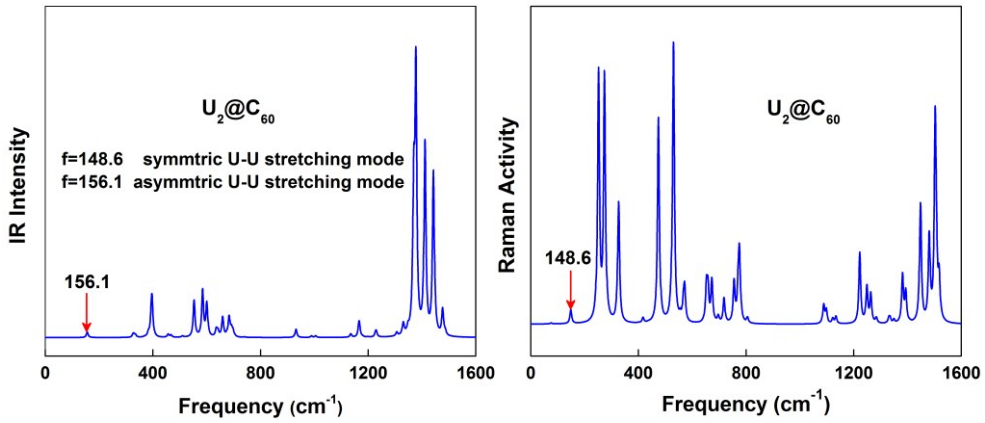

Figure S1. IR and Raman spectra of $U_2@C_{60}$ at PBE/SEG_ECP60MWB~6-31G (d) level.

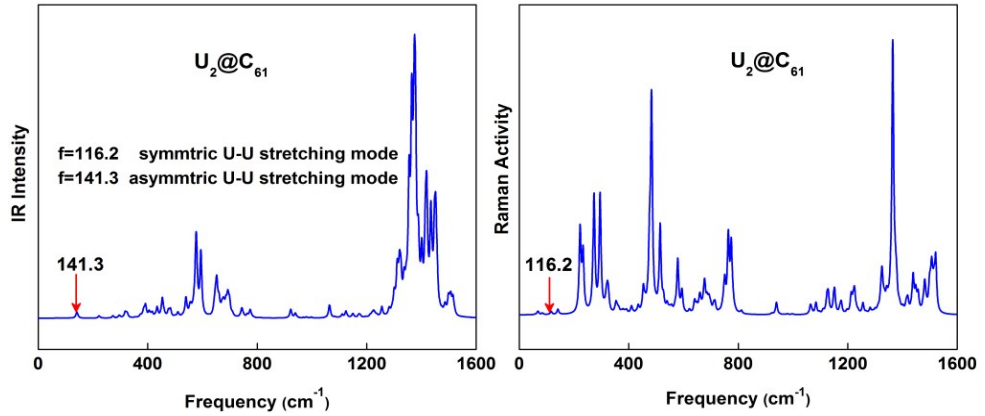

Figure S2. IR and Raman spectra of $U_2@C_{61}$ at PBE/SEG_ECP60MWB~6-31G (d) level.

Part 3. Relative energy calculations for UHe@C_{60} using ZORA approach.

Table S3. Relative energy calculations for UHe@C_{60} using ZORA approach.

Method	ΔE (eV)			
	Singlet	Triplet	Quintet	Septet
SR	0.29	0	0.72	1.28
SOC	2.83	0	0.03	9.70

Combined with the Table S1, we found that RECP and ZORA approach have the consistent results, namely, the ground state is triplet. It is showed that the spin-orbit coupling has no qualitatively influence on the results in this system, which further verifies the reliability of our calculated results.

Part 4. Molecular dynamics simulations of UHe@C_{60}

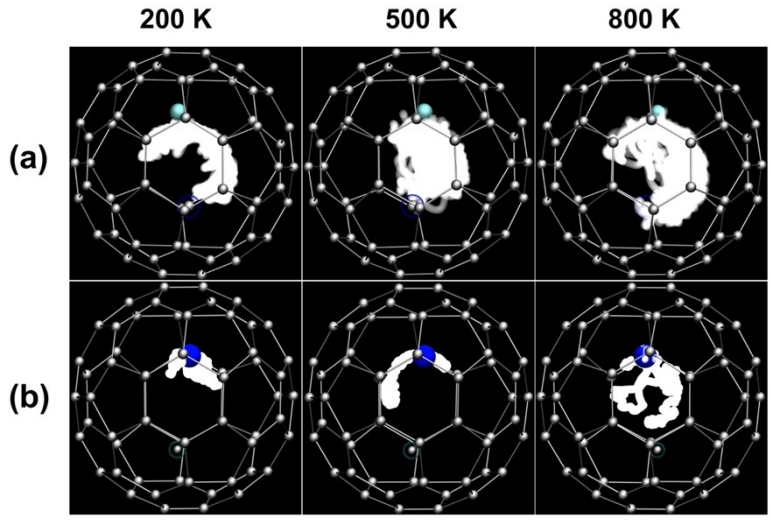

Figure S3. The MD trajectories of He and U atoms inside the C_{60} fullerene at different temperatures (200 K, 500 K and 800 K). The diagrams (a) and (b) demonstrate the trajectories of He and U atoms, respectively. Atom color are shown: U (blue), C (gray), He (cyan). In order to highlight target atom, so corresponding U and He atoms in (a) and (b) are represented in transparent, respectively.

We performed an annealing MD simulation at DFT-PBE level. At high temperature, the carbon cage is vibrating, but the structure is not broken, He and U are rotating in the cage. At low temperature, the location of U and He are both around the hexagonal centers which is in line with the geometry optimization results. It can be seen that the U atom in cage only move slightly, while the He has remarkably larger movement amplitude. Thus, we display the two curves both energy vs. time and Root-Mean-Square-Deviation (RMSD) vs. time for UHe@C_{60} at low temperature. Since these information are more important and can further help us for understanding the UHe@C_{60} system.

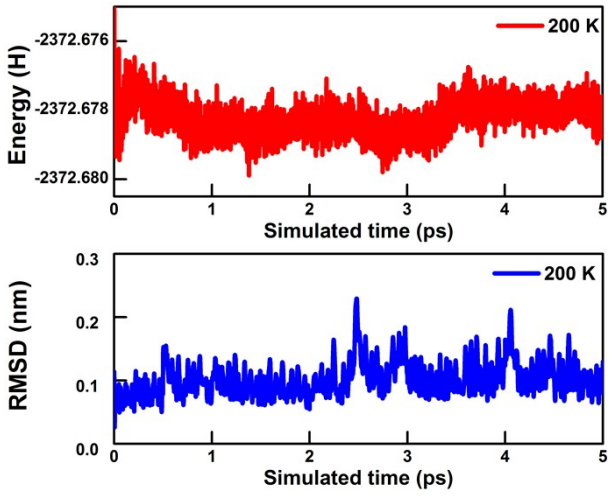

Figure S4. Energy vs. time and RMSD vs. time for UHe@C_{60} system in 200 K.

Part 5. Charge distribution and spin population of UHe@C_{60} and U@C_{60}.

Table S4. Charge distribution (e) and spin population (e) of UHe@C_{60} and U@C_{60}.

	UHe@C_{60} (U@C_{60})[a]				
	Charge (e)			Net spin (e)	
	NPA	Hirshfeld	Milliken	Mulliken	Hirshfeld
U	0.52(0.76)	0.47(0.52)	0.41(0.48)	2.21(2.25)	2.03(2.09)
C	-0.66(-0.76)	-0.58(-0.52)	-0.49(-0.48)	-0.21(-0.25)	-0.04(-0.09)
He	0.15	0.11	0.08	0	0
Total	/	/	/	2.00(2.00)	2.00(2.00)

[a]The results for U@C_{60} are also included in brackets.

Part 6. Contour maps of electron density difference of UHe@C_{60}

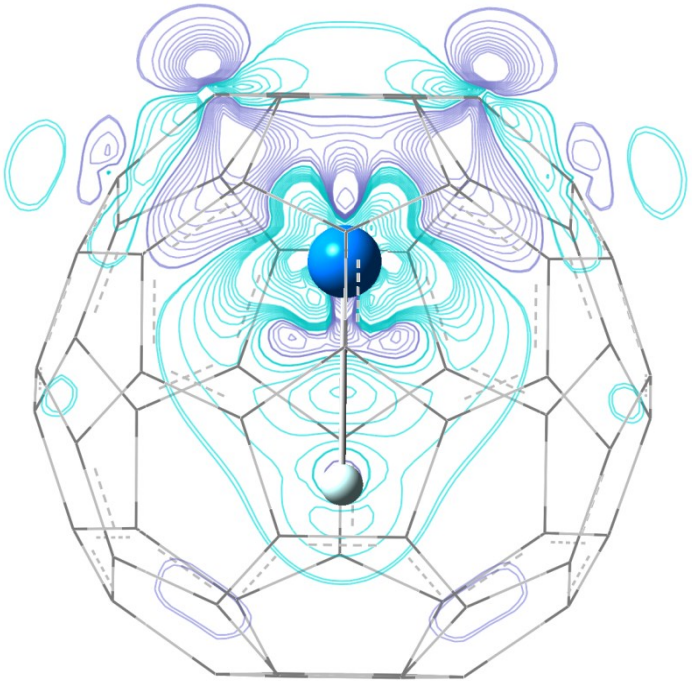

Figure S5. Contour maps of electron density difference. The density differences is obtained by subtracting electron density of isolated U, He and C_{60} from that of UHe@C_{60}. The purple lines and green lines show the charge accumulation and depletion, respectively.

In order to further investigate the interaction between He and U@C_{60}, we observe the electron gains and losses using electron density difference. As seen in Figure S5,

U and He are surrounded by blue lines, and cage is surrounded by purple lines, which demonstrates the electron depletion and accumulation, respectively. We can see that there is no electrons accumulation either between He and U/fullerene cage. On the other hand, the purple area between U and C atoms indicates U transfer electron to carbon cage. It also demonstrates the presence of covalent interaction between them.

Part 7. Detailed data of energy decomposition analysis for UHe@C_{60} system.

Table S5. Energy decomposition analysis of UHe@C_{60} system (energy in eV).

System	ΔE_{int}[a]	ΔE_{pauli}[b]	$\Delta E_{elestat}$[c]	ΔE_{orb}[d]
UHe@C_{60}	0.10	0.65	-0.21	-0.34

[a]Interaction energy, $\Delta E_{int} = \Delta E_{Pauli} + \Delta E_{elestat} + \Delta E_{orb}$; [b]Pauli repulsion energy; [c]Electrostatic interaction energy; [d]Orbital interaction energy. Within this energy decomposition scheme the attractive and repulsive terms are negative and positive, respectively.

Part 8. Detailed data of TD-DFT calculations for UHe@C_{60}.

Table S6. TD-DFT excitation energies (E in eV), excitation wavelengths (λ in nm), oscillator strengths (f, only energies with f > 0.01 are shown) and weights of UHe@C_{60} (only contribution > 10% are shown).

E / λ	f	Transitions
1.600\774.88	0.012	75% HOMOα-1[C 2*s* 1.07%, 2*p* 29.49%;U 5*f* 66.38%] → LUMO+6[C 2*p* 86.06%;U 5*f* 9.62%] 16% HOMOα [C 2*p* 22.12%;U 5*f* 73.34%] →LUMOα+6
1.603\773.65	0.012	75% HOMOα-1 →LUMOα+7 [C 2*p* 86%;U 5*f* 9.71%] 16% HOMOα →LUMOα+7
1.612\768.95	0.015	12% HOMOα-3[C 2*s* 1.63%, 2*p* 61.65%;U 5*f* 35.28%] →LUMOα+1[C 2*p* 31.27%;U 5*f* 61.99%] 16% HOMOα-3 →LUMO α +3 [C 2*p* 39.73%;U 6*d* 2.24%, 5*f* 52.45%] 11% HOMOα-2[C 2*s* 1.62%, 2*p* 61.57%;U 5*f* 35.35%] →LUMOα[C 2*p* 30.96%;U 5*f* 62.24%] 17% HOMOα-2 →LUMO α +4 [C 2*p* 39.20%;U 6*d* 2.13%, 5*f* 52.08%]
2.034\609.58	0.005	55% HOMOα-8[C 2*p* 95.43%;U 5*f* 3.39%]→LUMOα

		20% HOMOα-7[C 2*p* 95.43%;U 5*f* 3.40%]→ LUMOα+1
2.160\574.25	0.004	26% HOMOα-8→LUMOα+4 24% HOMOα-7→ LUMOα+3 45% HOMOα-4[C 2*p* 96.30%;U 5*f* 2.83%]→ LUMOα+4
3.234\383.41	0.019	14% HOMOα-15[C 2*s* 1.04%, 2*p* 94.63%; U 5*f* 2.89%] →LUMOα+2[C 2*p* 56.07%; U 5*f* 37.77] 13% HOMOα-11[C 2*p* 95.21%; U 5*f* 2.93%] →LUMOα+3 13% HOMOα-9[C 2*p* 98.86%;U 5*f* 0.1%] →LUMOα+5
3.234\383.36	0.020	16% HOMOα-14[C 2*s* 1.04%, 2*p* 94.64%;U 5*f* 2.89%] →LUMOα+2 22% HOMOα-12[C 2*s* 1.05%,2*p* 90.31%;U 5*f* 8.15%;] →LUMOα+1 17% HOMOα-11 →LUMOα+4 12% HOMOα-10[C 2*p* 98.87%] →LUMOα+5[C2 *p* 35.70%;U 5*f* 58.89%] 12% HOMOα-2 →LUMOα+14[C 2*s* 6.14.%, 2*p* 94.49%]
3.244\382.24	0.035	36% HOMOα-13[C 2*s* 1.05%, 2*p* 94.86%; U5*f* 2.32%] →LUMOα+2 14% HOMOα-11 →LUMOα+2
3.272\378.90	0.012	12% HOMOα-13 →LUMOα 60% HOMOα-12 →LUMOα+1
3.272\378.88	0.013	13% HOMOα-13 →LUMOα+1 35% HOMOα-12 →LUMOα 21% HOMOα-13 →LUMOα+1 12% HOMOα-9 [C 2*p* 98.86%]→LUMOα+5
3.285\377.49	0.025	24% HOMOα-12 →LUMOα+5 41% HOMOα-1→LUMO+17[He 1*s* 1.10%; C 2*s* 1.75%, 2*p* 4.57%;U 7*s* 64.59%;]

3.437\360.69	0.014	17% HOMOα-15 →LUMOα+1 25% HOMOα-15 →LUMOα+3 11% HOMOα-14 →LUMOα 20% HOMOα-14 →LUMOα+4 23% HOMOα-13 →LUMOα+2
3.560\348.25	0.027	20% HOMOα-15 →LUMOα+3 42% HOMOα-14 →LUMOα+4 18% HOMOα-12 →LUMOα+5

Part 9. Infrared and Raman spectra of UHe@C_{60} and U@C_{60}

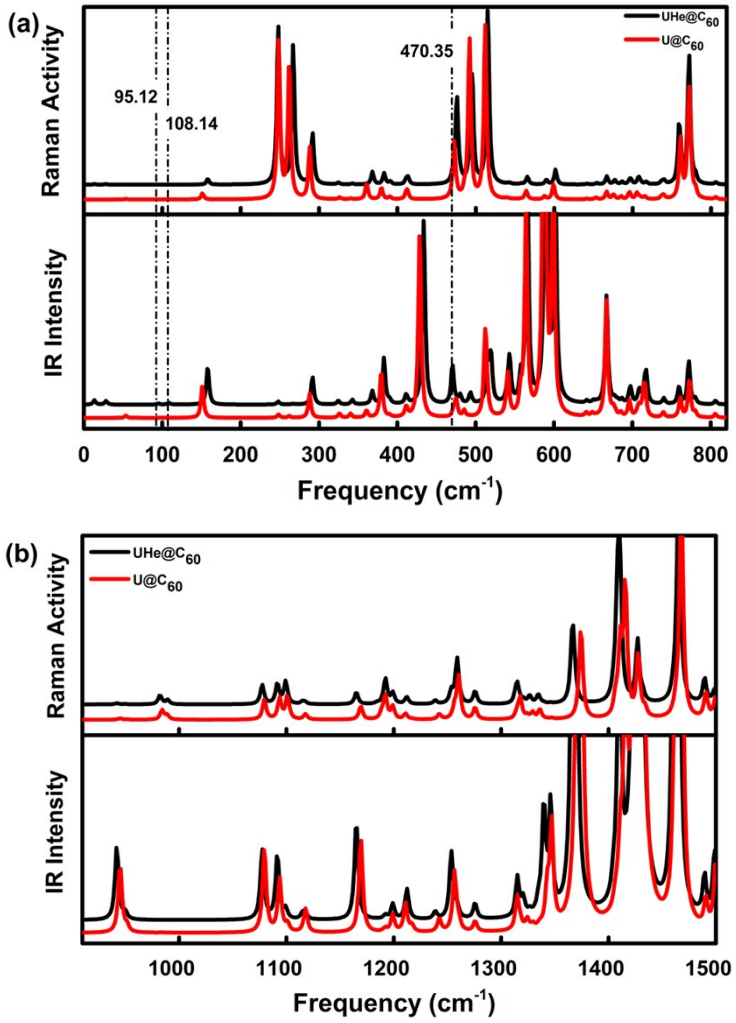

Figure S6. Infrared and Raman Spectra of UHe@C_{60} and U@C_{60}, which are shown in black and red lines, respectively. Compared UHe@C_{60} with U@C_{60}, three new characteristic peak positions have been pointed out by dotted lines.